

Received December 28, 2019, accepted January 27, 2020, date of publication February 13, 2020, date of current version March 10, 2020.

Digital Object Identifier 10.1109/ACCESS.2020.2973664

# 3D Printed Elastomeric Lattices With Embedded Deformation Sensing

CAROLYN CARRADERO SANTIAGO<sup>1</sup>, CHRISTIAAN RANDALL-POSEY<sup>2</sup>,  
ANDREI-ALEXANDRU POPA<sup>3</sup>, LARS DUGGEN<sup>4</sup>, BRIAN VUKSANOVICH<sup>2</sup>,  
PEDRO CORTES<sup>4</sup>, AND ERIC MACDONALD<sup>5</sup>, (Senior Member, IEEE)

<sup>1</sup>Materials Science and Engineering Department, Youngstown State University, Youngstown, OH 44455, USA

<sup>2</sup>Mechanical Engineering Department, Youngstown State University, Youngstown, OH 44455, USA

<sup>3</sup>Mechatronics Department, University of Southern Denmark, 80523 Odense, Denmark

<sup>4</sup>Department of Civil/Environmental and Chemical Engineering, Youngstown State University, Youngstown, OH 44455, USA

<sup>5</sup>Electrical and Computer Engineering Department, Youngstown State University, Youngstown, OH 44455, USA

Corresponding author: Carolyn Carradero Santiago (ccarradero@student.yzu.edu)

This work was supported in part by the Friedman Endowment for Manufacturing at Youngstown State University.

**ABSTRACT** New durable elastomeric materials are commercially available for 3D printing, enabling a new class of consumer wearable applications. The mechanical response of soft 3D printed lattices can now be tailored for improved safety and comfort by (a) leveraging functional grading and (b) customizing the outer envelope to conform specifically to the anatomy of the subject (e.g. patient, athlete, or consumer). Furthermore, electronics can be unobtrusively integrated into these 3D printed structures to provide feedback relating to athletic performance or physical activity. A proposed sensor system was developed that weaves unjacketed wires at two distinct layers in a lattice to form a complex capacitor; the capacitance increases as the lattice is compressed and can detect lattice deformation. A structure was fabricated and demonstrated with both static compression as well as low-velocity impact to highlight the utility for wearable applications. This work is focused on improving the performance of American football helmets as highlighted by the National Football League (NFL) Helmet Challenge Symposium; however, the lattice sensing concept can be extended to metal and ceramic lattices as well - relevant to the automotive and aerospace industries.

**INDEX TERMS** Additive manufacturing, lattices, elastomers, embedded sensing, Internet of Things.

## I. INTRODUCTION

Additive Manufacturing has been leveraged to fabricate form-and-fit prototypes in arbitrary geometries for decades. The integration of electronic components within these shapes has been pursued since the 1990s providing advances in antennas, biomedical devices, smart wearables, prosthetics, electromechanical devices, and satellites [1]–[12]. In 3D printed electronics, conductors serve as interconnect between embedded electronic components with a variety of methods including micro-dispensing, ink jetting and aerosol jetting of conductive inks [10], [13], [14] as well as by the structural embedding of bulk conductors inserted directly into additively-manufactured dielectric substrates [15], [16]. The integration of these 3D printed structures with electronics have three possible manufacturing strategies: (a) during fabrication with process interruptions, (b) after fabrication

with the insertion of components into structural cavities, or (c) after the fabrication with components interposed between two printed structures that are subsequently polymer over-molded together. Generally, 3D printed electronics have included process interruptions of the additive manufacturing for both the component placement and interconnect printing. Within the context of additive manufacturing, lattices are the focus of significant research as the structures since they (a) provide a tailored weight-versus-strength balance and (b) can be fabricated to include strut-size variation – gracefully modulating the density and mechanical response from one side to the other within the structure [17]–[21]. Introducing wires into these structures for the embedding of electronics seems to fit into aerospace applications in which light weighting is paramount. Other potential applications include wearable electronics, in which soft and resilient elastomers provide dampening for comfort and safety. In both applications, sensing in these structures provides unprecedented *internet-of-things* data acquisition for structural health monitoring

The associate editor coordinating the review of this manuscript and approving it for publication was Shaohua Wan<sup>1</sup>.



**FIGURE 1.** Printed shoe sole with lattices (photo from formlabs.com).

in aircraft or health and activity monitoring for the general public. Vat photopolymerization (VPP) is the original form of additive manufacturing out of the seven processes defined in the ISO/ASTM taxonomy [22]. The technology was commercialized by 3D Systems in the 1980s (and contemporaneously invented in Japan and France). VPP provides intricate features as photocuring is completed with the spatial resolution provided by a laser beam in most cases or by UV projection in others. The surface finish is also outstanding as the original feedstock is a liquid photopolymer in a vat. Although the materials are relegated to photochemistry, the material performance has steadily improved over the last four decades and the diversity of materials now includes durable elastomers with high coefficients of restitution, well suited for energy-return applications to improve athletic performance (e.g. running shoes). By tailoring the mechanical performance of these materials with lattice engineering, the VPP elastomer structures can be further enhanced for human application. Fig. 1 illustrates a sole printed for the New Balance shoe in which the insole was fabricated by Formlabs (Boston, USA). With embedded electronics, state-of-the-art 3D printed shape-to-fit wearables will be imbued with unprecedented programmable functionality.

Using standard vat photopolymerization and thermoplastic extrusion, previous work has demonstrated 3D printed electronics using both printed inks and embedded wires for interconnection [11], [14]–[16], [23]–[30]. Ink conductors can suffer from low conductivities as the curing temperature is limited by the max temperature of the polymer substrate; conductive inks have been used to connect components and sensors and provide substantial manufacturing flexibility (e.g. conformally deposited, etc.). This paper focuses on the second approach which includes weaving a pair of wires in adjacent unit-cell layers through an elastomer lattice in order to serve as a complex capacitor. The structure demonstrates the concept regardless of the method of conductor insertion.

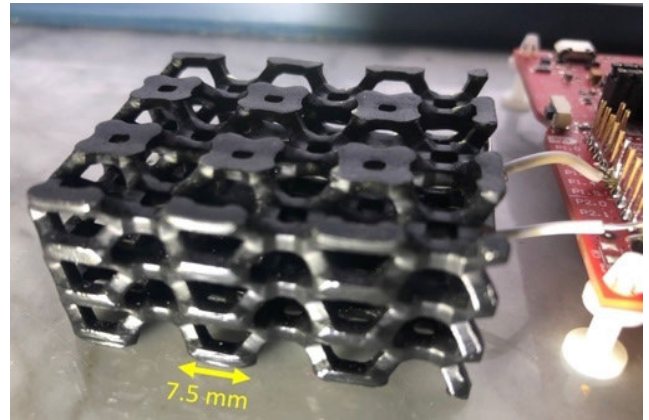


**FIGURE 2.** Elastomer lattice with electronics and the unobtrusive pair of wires acting as a sensor. The red board (MSP430 Launchpad) can be reduced to a single 5mm × 5mm chip with a coin battery. The polymer material is used in 3D-printed commercially available New Balance shoes.

The capacitor was measured with a relatively high sampling rate (250 Hz) and serves as a proxy for the dynamic deformation of the layer that separates the two wires.

## II. MATERIALS AND METHODS

This research effort was focused on providing a proof of concept of the combination of high-coefficient-of-restitution elastomer lattices infused with an accurate, high-response-rate sensor. The material is a proprietary photocurable polymer targeting a printed commercial shoe and printed by Formlabs. Any printable elastomer could have been used in this experiment, but the Rebound material [31] was particularly interesting due to the natural application as insole for a shoe.

### A. LATTICE DESIGN WITH EMBEDDED CAPACITIVE SENSOR

Lattices have attracted substantial attention in recent research as additive manufacturing can fabricate these structures more easily than traditional methods. Modulating the density of the structures by varying strut or beam size throughout the lattice has been achievable by the combination of AM and advances in CAD software, both of which have dramatically improved particularly for generating complex geometries. Many lattice unit cells have been explored for optimizing stiffness or compression performance while minimizing the overall weight of the structure [19], [32]–[37] and the exploration has included functionally-graded lattices that can modulate the effective density for tailoring the mechanical and electromagnetic response [34], [37]–[40]. In this study, a simple uniform hexagonal lattice was used (50 mm × 50 mm × 24 mm to replicate an internal pad within a typical American football helmet). Figure 2 shows the lattice that was designed – primarily for the subjective sense of comfort for human contact in the context of the Rebound material. Furthermore, the hexagonal unit cell provided a self-aligning collection point for the wires. An intentional design feature, triangular notches are in the voids of each cell, and the wires

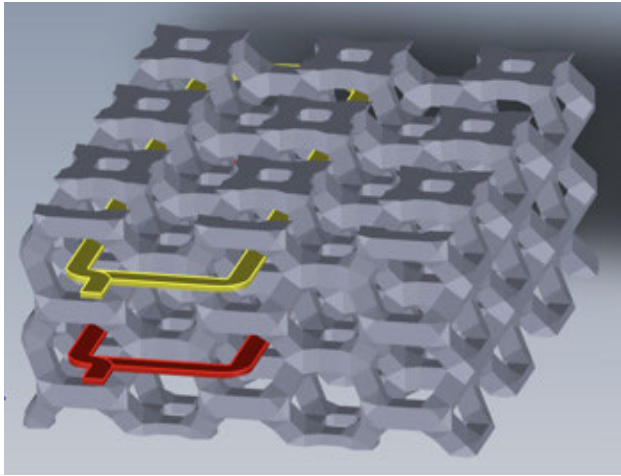


**FIGURE 3.** Measured configuration Isometric (A) views of two wires forming a capacitor in the measured configuration. The yellow wire is the top plate and the red is the bottom plate of a capacitor. The gray is a dielectric elastomer lattice, the deformation of which can be indirectly determined by measuring the capacitance.

naturally settled at the midpoint of the cell when pulled tight. By placing wires at two levels – both precisely in the middle of each layer – the pair of wires were separated by the consistent height of a single cell, midpoint to midpoint (7.5 mm). Furthermore, the lattice had a large see-through void to facilitate the ease of weaving wires at either layer. Only one type of lattice was considered as the interest focused on the response of the capacitance sensor rather than on the mechanical performance of the lattice configuration. Further research is being performed on different lattice arrangements to test their dynamic performance. To form a woven capacitor within the lattice (Fig. 3), the configuration of both wires through the lattice must be identical in the X-Y plane to accumulate as much “sensing” capacitance as possible. In this case, changes in the sensor capacitance directly translate into deformation. The capacitance of the wires outside of the lattice is extraneous and dilutes the measurements and decreases the sensitivity. The actual wire route can enable the monitoring of the deformation in arbitrary sections of the lattice including specific cells, quadrants, rows, columns and even the average deformation of the entire layer (see fig. 4). Moreover, the capacitors can be placed on horizontal planes as shown in this study, but also, in vertical planes as well - and any combination of the two to provide diagonal deformation measurement. The only recommendation is that the spacing distance between the wires be maintained as the pair of wires travel through the lattice, otherwise, the regions with closer sections will contribute more to the sensor capacitance, and therefore, exert an increased influence on the measured value.

**B. INEXPENSIVE AND EMBEDDABLE CAPACITANCE MEASUREMENT**

The capacitance that forms between the pair of wires is proportional to the length of the routes and inversely proportional to the height of the unit cell that separates the

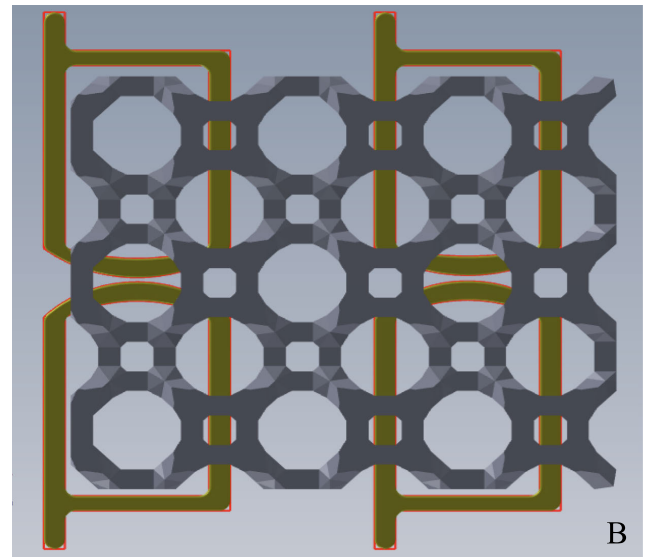
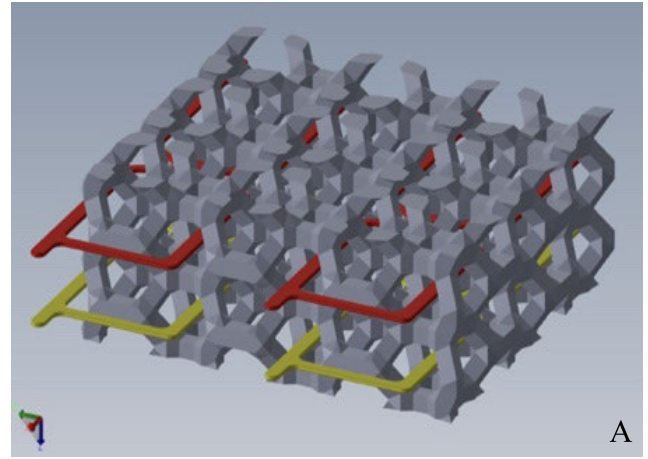


**FIGURE 4.** Isometric (A) and bottom view (B) and of a lattice with an alternative configuration in four quadrants for selective sensing. The selectivity can be extended to any combination of cells in both vertical and horizontal configurations.

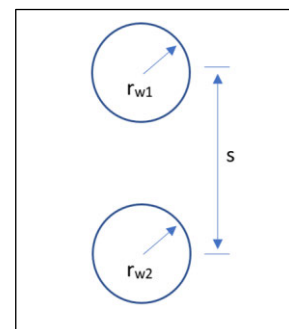


**FIGURE 5.** Schematic used to calculate the sensor capacitance.

wires. Fig. 5 shows the cross section of the two wires that form a capacitance which increases with accumulation of the length of the wires. The capacitance is also proportional to the permittivity of the dielectric which in this case is a mixture of the elastomer and air. This project measured the



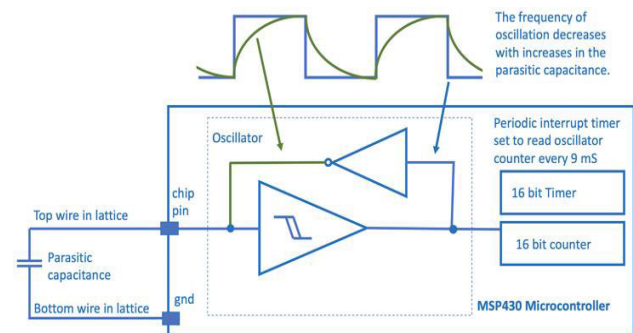


FIGURE 6. Oscillator-based capacitance measurement.

relative capacitance between the wires to serve as a proxy for deformation. By using a relaxation oscillator, the number of oscillations per any 4.0 ms period provided an inverse of the capacitance and a value linearly proportional to the distance between the wires as shown in Fig. 5 and described by equation (1). The 4.0 ms period allowed for a good compromise between displacement resolution and sampling rate. The plate-capacitor assumption is only approximate, as the wire shape used in the study has a comparatively large amount of fringing fields which changes the effective overlap area between the electrodes [41]. One inexpensive approach for embedding the measurement electronics directly into the lattice includes the Texas Instruments MSP430G2553 with fully integrated capacitive sensing – a chip that only requires an additional battery and the two sensor wires. The chip includes an internal relaxation oscillator that is “slugged” by increases in the external capacitance which increases as the pair of wires are compressed together. The circuit oscillates fewer times during a precise duration as determined by a periodic interrupt and a counter is used to count the number of oscillations between the periodic timer interrupts. Figure 6 shows the schematic for the basic circuit used; here, the data was transferred with a virtual serial port through a USB cable to a computer for analysis and graphing, but the data acquisition could easily be enhanced with a wireless radio protocol like Bluetooth. Additionally, two LEDs (red and green) were also used to indicate when a binary threshold of compression was detected, and this could be further enhanced by blinking the LED with a frequency proportional to the amount of the single-layer displacement. This indication could be used for identifying an athlete that may be injured during a game or marathon - due to excessive accelerations.

$$C = \frac{2\pi l \epsilon_0 \epsilon_r}{\cosh^{-1} \left( \frac{s^2 - r_1^2 - r_2^2}{2r_1^2 r_2^2} \right)} \quad (1)$$

### C. QUASI-STATIC LOADING

Compression tests were conducted on a Universal Instron machine 5500R at a loading rate of 2.0 mm/min at room temperature. Here, the lattice system was placed between two flat fixtures and during the testing the capacitance was captured on a laptop connected to the MSP430 through an

emulated serial port using a USB cable. The lattice structure was subjected to consecutive loading and unloading cycles to ensure repeatability in the system.

### D. DYNAMIC IMPACT WITH HIGH SPEED VIDEO

Low velocity impact tests were performed on a falling-weight impact tower using a mass of 4.25 kg dropped at four different heights: 50, 100, 200 and 400 mm. The impact tests were recorded at 2000 frames per second providing a temporal resolution of 500  $\mu$ s using a high-speed video camera (Olympus i-Speed3). The capacitance measurement was performed at 4mS sampling. By synchronizing the data measurements with the high-speed video which showed the physical distance between layers, the sensor accuracy was evaluated. Furthermore, the low-velocity impact provided an assessment of the durability of the lattice with the embedded sensor.

## III. RESULTS AND DISCUSSION

Both quasi-static compression and dynamic impact testing were explored to evaluate the accuracy of the capacitive sensing to measure the extent of deformation. The tests were repeated, and it was observed that the lattice shape returned to the original form after the quasi static compression tests. Similarly, when subjecting the part to dynamic testing, the sensor and the lattice immediately returned to the original form.

### A. QUASI-STATIC TESTING

The quasi-static testing evaluated sensitivity and accuracy of the sensor. The lattice was compressed at 2.0 mm/min until reaching a compression force of 500 N, which represented a lattice displacement of 12 mm. The value of 500 N was considered based on previous research performed on impact forces experienced on shoes during running [42]. The capacitance measured in this test was used as a proxy for the compression displacement of the measured single cell layer (7.5 mm thick). Figure 7 shows the recorded displacement from the Instron and the capacitance sensor after subjecting the part to a limit of 500N. The figure shows the linear displacement of the Instron machine at rate of 0.033mm/S, which correspond to the loading rate of 2.0 mm/min used during the testing. This displacement is associated to the constant compressive extension applied to the entire lattice structure. The right axis of both figure 7 A and B are linearized functions which translated the measured relaxation oscillator cycles to the extent of deformation. The cycles are inversely proportional to the capacitance which is inversely proportional to the distance between the capacitor plates. Consequently, the cycles can be linearly and directly converted to the magnitude of deformation starting from no deformation (zero load) and ending in the deformation for the maximum load, a distance of 3.5 mm as measured from image analysis. In contrast, the capacitance sensor shows an exponential profile during the testing but is limited to a particular layer only. Here, it was observed that during the initial compression, most of the displacement took place on the top and bottom of the lattice part, with a reduced extension

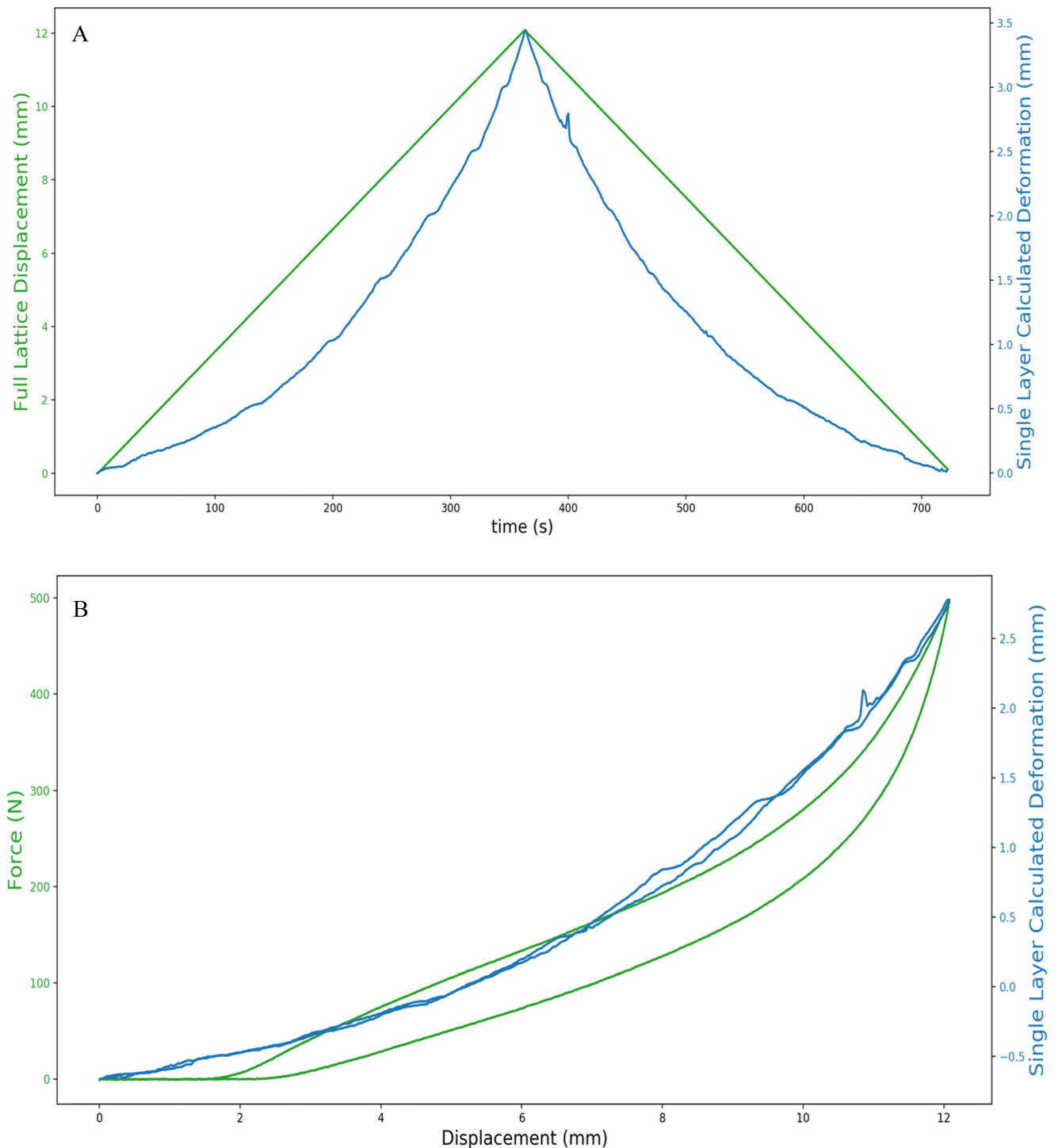


**FIGURE 7.** (A) Quasi-static compression (2 mm/minute) to 500 N. Green is full lattice deformation with a return after reaching the limit force. Blue is the calculated single layer deformation based on the capacitance measured for that layer. (B) Force and Calculated Layer Height (based on capacitance measurement) versus Full Lattice Deformation.

at the center of the structure where the sensor was placed (see Fig. 8). As the testing continued, the central part of the lattice was exposed to a larger displacement, resulting in a rapid deformation on the sensor as shown in Fig. 7A. A full load-unload cycle under a loading rate of 2.0 mm/min is

shown in Fig. 7B. The figure shows a typical non-linear elastic and viscoelastic behavior accompanied by an energy dissipation profile displayed by the hysteresis loop; characteristics commonly observed on elastomers [43]. Indeed, this type of behavior is known from both electrical and mechanical

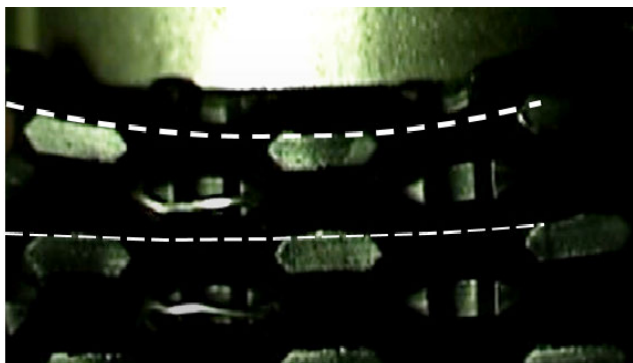


**FIGURE 8.** Compression testing showing a larger deformation at the center of the lattice where the sensor was located [47].

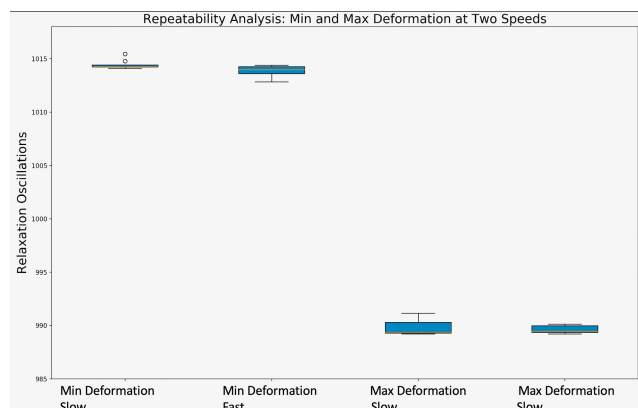


**FIGURE 9.** Box plot of repeatability analysis for two cycling speeds.

systems and has been extensively studied on several models [44]–[46]. Included in the figure is the calculated deformation from the capacitance sensor, where it is observed that the system displays a minimal hysteresis, since no mechanical loads were imposed on the wires.

To evaluate the variation of the sensor data, a thousand measurements were acquired with zero load and the average measurement from the relaxation oscillator was 1014.72 cycles with a standard deviation of 0.758, which is less than 1% variation in a static state. For repeatability analysis, 10 quasi-static tests were completed at both (a) 2.0 mm per minute and (b) 20.0 mm per minute (shown in fig. 9). In both cases, the test was performed until reaching a load of 500 N, followed by an unloading cycle. The box plot shows the relaxation oscillation values (serving as a proxy for capacitance and consequently deformation) for both slow (2.0 mm/min) and fast velocity (20.0 mm/min) and at both the minimum and maximum deformation. For all cases, the values were repeatable to less than 1% and the speed of the load cell had no impact on the measured value. The lattice returned to the original position and the sensor confirmed the elastic behavior.

### B. DYNAMIC TESTING

The lattice structure was subjected to a series of impact velocities ranging from 1.0 to 2.8 m/s. Here, the lattice deformation was recorded on a high-speed video camera. From the video,



**FIGURE 10.** High-Speed video of two different drop tests: 50 mm [1 m/s] (A), 100 mm [1.4 m/s] (B). The frame in each case shows the moment of maximum compression [47].

the frame associated with the maximum compression at a given drop height was identified (see fig. 10). The wires on the lattice were visible in the video, and therefore the distance between them at their closest points was measured in terms of the number of pixels. For each video, prior to impact, the pixel difference between the visible wires at each layer is measured to provide the uncompressed case. Then, a frame in each video was identified that included the pixel distance was 193 and correlated to the full unit cell height of 7.5 mm - for approximately 38 microns per pixel on the front surface of the lattice given the lattice size and camera position. The capacitance measurement was inversely proportional to the distance between the wires which represents the capacitor plate thickness. For this project, the calculated distance was normalized for the uncompressed case. Figure 11 shows a normalized representation of the deformation from the pixel heights in the videos and the normalized proxy for the capacitance measured between the two woven wires and distinct layers. From the figure, it is observed that both profiles show similar trends. The figure also shows that the sensor is sensitive enough for recording diverse impact energies. Indeed, at an impact energy of 16.6 J, the sensor recorded a deformation two times larger than the recorded at 2.1 J. This clearly highlights the potential applications of this

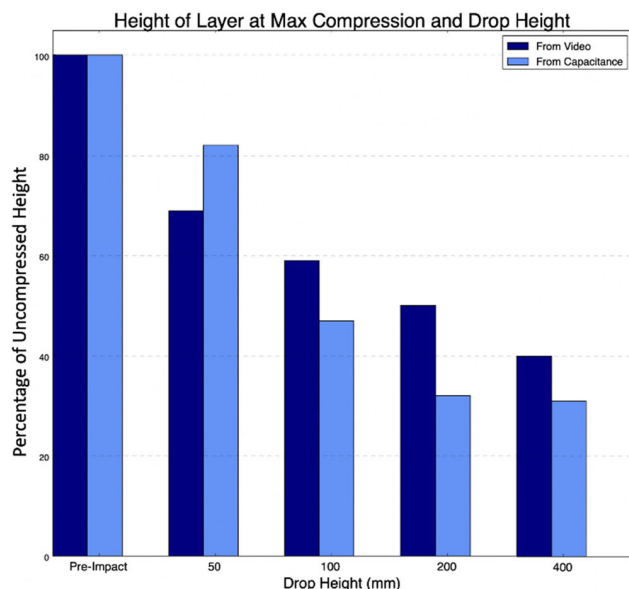


**FIGURE 11.** Pixel height and capacitance proxy serving to measure compressive deformation.

inexpensive sensor to be used on high impact energy conditions as those found on contact sports such as American football.

#### IV. CONCLUSION

A sensorized elastomer lattice was demonstrated; it was shown that the sensor measures both high-performance mechanical response while exhibiting accurate static measurement of deformation and reasonable low-velocity impact sensing. By combining both the mechanical benefits of lattice structures coupled with embedded intelligence and sensing, new anatomy-specific smart wearables are now achievable. The elastomer material used in this work is durable, and consequently, the resulting structures require sensors and electronics fabricated and integrated in novel manners to survive in harsh environments. By increasing the sampling rate of the data acquisition, the response of the system can be improved; however, the current implementation with 4.0 ms sampling was sufficient for low-velocity applications that might be typically experienced in the soles of shoes while running. Significantly more repeatability analysis is required for applications such as shoes which would require hundreds of thousands of cycles of compression. However, this proof of concept leveraged a peripheral development board (MSP430 Launchpad), and consequently, the connections were not ruggedized. The future work of this research will focus on miniaturization including the integration of a single unpackaged silicon die (microcontroller) as well as a coin cell battery for power. As electronic components generally require rigid substrates, a small stiff 3D printed insert will be populated with electronics and then unobtrusively overmolded into a cavity in the lattice. The system (lattice through a microcontroller) will be tested at higher impact energies, such as those recorded on full contact sports such as an open field tackle in

American football, and the full integration of electronics into the lattice to avoid interference with the activity. Data transfer will be enhanced by including wireless communications with a protocol such as Bluetooth or Zigbee.

#### ACKNOWLEDGMENTS

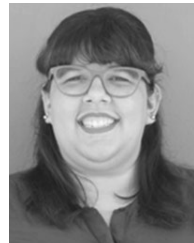
The authors would like to thank the Office of Research and the Friedman Endowment for supporting this work at Youngstown State University. The authors are also grateful to Lizz Hill from Formlabs, who kindly supplied the rebound lattices used on this research work

#### REFERENCES

- [1] C. M. Shemelya, M. Zemba, M. Liang, D. Espalin, C. Kief, H. Xin, R. B. Wicker, and E. W. MacDonald, "3D printing multi-functionality: Embedded RF antennas and components," in *Proc. 9th Eur. Conf. Antennas Propag. (EuCAP)*, Apr. 2015, pp. 1–5.
- [2] E. MacDonald and R. Wicker, "Multiprocess 3D printing for increasing component functionality," *Science*, vol. 353, no. 6307, Sep. 2016, Art. no. aaf2093
- [3] M. S. Mannoor, Z. Jiang, T. James, Y. L. Kong, K. A. Malatesta, W. O. Soboyejo, N. Verma, D. H. Gracias, and M. C. McAlpine, "3D printed bionic ears," *Nano Lett.*, vol. 13, no. 6, pp. 2634–2639, Jun. 2013.
- [4] F. B. Prinz, L. E. Weiss, and D. P. Siewiorek, "Electronic packages and smart structures formed by thermal spray deposition," U.S. Patent 5 278 442, Jan. 11, 1994.
- [5] K. B. Perez and C. B. Williams, "Combining additive manufacturing and direct write for integrated electronics—A review," in *Proc. 24th Int. Solid Freeform Fabr. Symp.—Additive Manuf. Conf. (SFF)*, 2013, pp. 962–979.
- [6] W. M. Marshall, J. D. Stegeman, M. Zemba, E. MacDonald, C. Shemelya, R. Wicker, A. Kwas, and C. Kief, "Using additive manufacturing to print a CubeSat propulsion system," in *Proc. 51st AIAA/SAE/ASEE Joint Propuls. Conf.*, Jul. 2015, p. 4184.
- [7] L. J. Love, R. F. Lind, and J. F. Jansen, "Mesofluidic actuation for articulated finger and hand prosthetics," in *Proc. IEEE/RSJ Int. Conf. Intell. Robots Syst.*, Oct. 2009, pp. 2586–2591.
- [8] E. Aguilera, J. Ramos, D. Espalin, F. Cedillos, and D. Muse, "3D printing of electro mechanical systems," in *Proc. Solid Freeform Fabr. Symp.*, 2013, pp. 950–961.
- [9] E. Macdonald, R. Salas, D. Espalin, M. Perez, E. Aguilera, D. Muse, and R. B. Wicker, "3D printing for the rapid prototyping of structural electronics," *IEEE Access*, vol. 2, pp. 234–242, 2014.
- [10] J. A. Paulsen, M. Renn, K. Christenson, and R. Plourde, "Printing conformal electronics on 3D structures with Aerosol Jet technology," in *Proc. Future Instrum. Int. Workshop (FIIW)*, Oct. 2012, pp. 1–4.
- [11] J. Hoerber, J. Glasschroeder, M. Pfeffer, J. Schilp, M. Zaeh, and J. Franke, "Approaches for additive manufacturing of 3D electronic applications," *Procedia CIRP*, vol. 17, pp. 806–811, 2014.
- [12] C. Shemelya, F. Cedillos, E. Aguilera, E. Maestas, J. Ramos, D. Espalin, D. Muse, R. Wicker, and E. MacDonald, "3D printed capacitive sensors," in *Proc. IEEE SENSORS*, Nov. 2013, pp. 1–4.
- [13] M. Mirzaee, S. Noghianian, L. Wiest, and I. Chang, "Developing flexible 3D printed antenna using conductive ABS materials," in *Proc. 2015 IEEE Int. Symp. Antennas Propag. USNC/URSI Nat. Radio Sci. Meeting*, Jul. 2015, pp. 1308–1309.
- [14] T. Rahman, L. Renaud, D. Heo, M. Renn, and R. Panat, "Aerosol based direct-write micro-additive fabrication method for sub-mm 3D metal-dielectric structures," *J. Micromech. Microeng.*, vol. 25, no. 10, Oct. 2015, Art. no. 107002.
- [15] D. Espalin, D. W. Muse, E. MacDonald, and R. B. Wicker, "3D Printing multifunctionality: Structures with electronics," *Int. J. Adv. Manuf. Technol.*, vol. 72, nos. 5–8, pp. 963–978, May 2014.
- [16] C. Kim, D. Espalin, M. Liang, H. Xin, A. Cuaron, I. Varela, E. Macdonald, and R. B. Wicker, "3D printed electronics with high performance, multi-layered electrical interconnect," *IEEE Access*, vol. 5, pp. 25286–25294, 2017.
- [17] F. N. Habib, P. Iovenitti, S. H. Masood, and M. Nikzad, "Fabrication of polymeric lattice structures for optimum energy absorption using Multi Jet Fusion technology," *Mater. Des.*, vol. 155, pp. 86–98, Oct. 2018.



- [18] M. Mazur, M. Leary, M. McMillan, S. Sun, D. Shidid, and M. Brandt, "Mechanical properties of Ti6Al4V and AlSi12Mg lattice structures manufactured by Selective Laser Melting (SLM)," in *Laser Additive Manufacturing*. Cambridge, U.K.: Woodhead Publishing, 2017, ch. 5, pp. 119–161.
- [19] S.-I. Park, D. W. Rosen, S.-K. Choi, and C. E. Duty, "Effective mechanical properties of lattice material fabricated by material extrusion additive manufacturing," *Additive Manuf.*, vols. 1–4, pp. 12–23, Oct. 2014.
- [20] A. Panesar, M. Abdi, D. Hickman, and I. Ashcroft, "Strategies for functionally graded lattice structures derived using topology optimisation for Additive Manufacturing," *Additive Manuf.*, vol. 19, pp. 81–94, Jan. 2018.
- [21] B. Gorny, T. Niendorf, J. Lackmann, M. Thoene, T. Troester, and H. J. Maier, "In situ characterization of the deformation and failure behavior of non-stochastic porous structures processed by selective laser melting," *Mater. Sci. Eng., A*, vol. 528, no. 27, pp. 7962–7967, Oct. 2011.
- [22] *ISO/ASTM 52900: 2015 Additive Manufacturing-General Principles-Terminology*, Standard ASTM F2792-10e1, 2012.
- [23] E. MacDonald, D. Espalin, and R. Wicker, "Connecting metal foils/wires and components in 3D printed substrates with wire bonding," U.S. Patent 20 170 225 273 A1, Aug. 10, 2017.
- [24] R. B. Wicker, E. MacDonald, F. Medina, D. Espalin, and D. W. Muse, "Extrusion-based additive manufacturing system for 3D structural electronic, electromagnetic and electromechanical components/devices," U.S. Patent 20 130 170 171 A1, Jul. 4, 2013.
- [25] M. O'Reilly and J. Leal, "Jetting your way to fine-pitch 3D interconnects," *Chip Scale Rev.*, vol. 14, no. 5, pp. 18–21, 2010.
- [26] P. Deffenbaugh, K. Church, J. Goldfarb, and X. Chen, "Fully 3D printed 2.4 GHz Bluetooth/Wi-Fi antenna," *Int. Symp. Microelectron.*, vol. 2013, no. 1, pp. 000914–000920, Jan. 2013.
- [27] R. Olivas, R. Salas, D. Muse, E. MacDonald, R. Wicker, M. Newton, and K. Church, "Structural electronics through additive manufacturing and micro-dispensing," *Int. Symp. Microelectron.*, vol. 2010, no. 1, pp. 000940–000946, Jan. 2010.
- [28] M. T. Rahman, J. McCloy, C. V. Ramana, and R. Panat, "Structure, electrical characteristics, and high-temperature stability of aerosol jet printed silver nanoparticle films," *J. Appl. Phys.*, vol. 120, no. 7, Aug. 2016, Art. no. 075305.
- [29] T. Seifert, E. Sowade, F. Roscher, M. Wiemer, T. Gessner, and R. R. Baumann, "Additive manufacturing technologies compared: Morphology of deposits of silver ink using Inkjet and aerosol jet printing," *Ind. Eng. Chem. Res.*, vol. 54, no. 2, pp. 769–779, Jan. 2015.
- [30] K. Church, E. MacDonald, P. Clark, R. Taylor, D. Paul, K. Stone, M. Wilhelm, F. Medina, J. Lyke, and R. Wicker, "Printed electronic processes for flexible hybrid circuits and antennas," in *Proc. Flexible Electron. Displays Conf. Exhib.*, Feb. 2009, pp. 1–7.
- [31] Formlabs. (Sep. 15, 2019). *Continuous Innovation From New Balance and Formlabs*. Accessed: Dec. 15, 2019. [Online]. Available: <https://formlabs.com/blog/new-balance-formlabs-continuous-innovation/>
- [32] A. Hussein, L. Hao, C. Yan, R. Everson, and P. Young, "Advanced lattice support structures for metal additive manufacturing," *J. Mater. Process. Technol.*, vol. 213, no. 7, pp. 1019–1026, Jul. 2013.
- [33] C. Chu, G. Graf, and D. W. Rosen, "Design for additive manufacturing of cellular structures," *Comput.-Aided Des. Appl.*, vol. 5, no. 5, pp. 686–696, Jan. 2008.
- [34] A. du Plessis, I. Yadroitsava, I. Yadroitsev, S. le Roux, and D. Blaine, "Numerical comparison of lattice unit cell designs for medical implants by additive manufacturing," *Virtual Phys. Prototyping*, vol. 13, no. 4, pp. 266–281, Oct. 2018.
- [35] E. Alabort, D. Barba, and R. C. Reed, "Design of metallic bone by additive manufacturing," *Scripta Mater.*, vol. 164, pp. 110–114, Apr. 2019.
- [36] L. Hao, D. Raymond, C. Yan, A. Hussein, and P. Young, "Design and additive manufacturing of cellular lattice structures," in *Proc. Int. Conf. Adv. Res. Virtual Rapid Prototyping (VRAP)*, 2011, pp. 249–254.
- [37] D. Mahmoud and M. Elbestawi, "Lattice structures and functionally graded materials applications in additive manufacturing of orthopedic implants: A review," *J. Manuf. Mater. Process.*, vol. 1, no. 2, p. 13, Oct. 2017.
- [38] M. Liang and H. Xin, "3D printed microwave and THz components," in *Proc. Asia-Pacific Microw. Conf. (APMC)*, vol. 2, Dec. 2015, pp. 1–3.
- [39] Z. Larimore, S. Jensen, A. Good, A. Lu, J. Suarez, and M. Mirotznik, "Additive manufacturing of Luneburg lens antennas using space-filling curves and fused filament fabrication," *IEEE Trans. Antennas Propag.*, vol. 66, no. 6, pp. 2818–2827, Jun. 2018.
- [40] M. Liang, W.-R. Ng, K. Chang, K. Gbele, M. E. Gehm, and H. Xin, "A 3-D Luneburg lens antenna fabricated by polymer jetting rapid prototyping," *IEEE Trans. Antennas Propag.*, vol. 62, no. 4, pp. 1799–1807, Apr. 2014.
- [41] C. R. Paul, *Analysis of Multiconductor Transmission Lines*. Hoboken, NJ, USA: Wiley, 2007.
- [42] K. O'Leary, K. A. Vorpahl, and B. Heiderscheidt, "Effect of cushioned insoles on impact forces during running," *J. Amer. Podiatric Med. Assoc.*, vol. 98, no. 1, pp. 36–41, Jan. 2008.
- [43] H. Cho, S. Mayer, E. Pösel, M. Susoff, P. J. in 't Veld, G. C. Rutledge, and M. C. Boyce, "Deformation mechanisms of thermoplastic elastomers: Stress-strain behavior and constitutive modeling," *Polymer*, vol. 128, pp. 87–99, Oct. 2017.
- [44] M. Ismail, F. Ikhouane, and J. Rodellar, "The hysteresis Bouc-Wen model, a survey," *Arch. Comput. Methods Eng.*, vol. 16, no. 2, pp. 161–188, Jun. 2009.
- [45] J. Vörös, "Modeling and identification of hysteresis using special forms of the Coleman–Hodgdon model," *J. Elect. Eng.*, vol. 60, no. 2, pp. 100–105, 2009.
- [46] G. Bertotti, "Dynamic generalization of the scalar Preisach model of hysteresis," *IEEE Trans. Magn.*, vol. 28, no. 5, pp. 2599–2601, Sep. 1992.
- [47] E. Macdonald and C. Carradero. *3D Printed Elastomer Lattices With Integrated Deformation Sensors*. LinkedIn. [Online]. Available: [https://www.linkedin.com/posts/eric-macdonald-06281b\\_youngstownstate-nfl-americanmakes-activity-6608702706754342912-Lhft](https://www.linkedin.com/posts/eric-macdonald-06281b_youngstownstate-nfl-americanmakes-activity-6608702706754342912-Lhft)



**CAROLYN CARRADERO SANTIAGO** was born in Caguas, Puerto Rico. She received the B.S. degree in physics and electronics from the University of Puerto Rico, Humacao, in 2017. She is currently pursuing the Ph.D. degree in materials science and engineering with the Youngstown State University. She has done research in several areas such as simulation of solar cells during her bachelor's in the University of Puerto Rico as well as in The Pennsylvania State University and Princeton University, simulating mixed matrices and engineering microwave circuits for quantum computing, respectively. Her current research works are focused on 3D printed wearable electronics, where she wants to integrate additive manufactured components that can be customized for a particular user with electronics for various applications such as sensing or feedback.



**CHRISTIAAN RANDALL-POSEY** was born in Pittsburgh, PA, USA, in 1997. He is currently a Senior undergraduate at Youngstown State University studying mechanical engineering. In 2018, he was a 2019–2020 recipient of the Thomas F. Mosure Scholarship and Chuck Joseph Football Scholarship.



**ANDREI-ALEXANDRU POPA** received the M.Sc. (Eng.) degree in mechatronics (modeling of dynamic mechatronic systems) from the Mads Clausen Institute (a part of the University of Southern Denmark), Sønderborg, Denmark. After working for one and a half years as a Research Assistant in the field of ultrasonic piezo-actuators, he reoriented toward additive manufacturing, being employed by the Mads Clausen Institute as an Engineer with extended responsibilities both within the field and from an educational perspective. He is currently a Mechatronics Engineer. Along with the maintenance and development of smart rapid prototyping facilities, he began his Ph.D. with the main objective of creating fully 3D-printed mechatronic products. This endeavor has since expanded to collaboration with Youngstown State University, Youngstown, OH, USA, with research efforts investigating properties and potential use-cases of 3D-printed overmolded wearable electronics.





His previous industry work includes defense, automotive manufacturing, and design for consumer products and industrial equipment.

**LARS DUGGEN** received the M.Sc. degree in mechatronics engineering and the Ph.D. degree in applied mathematical modeling from the University of Southern Denmark (SDU), Sønderborg, Denmark, in 2008 and 2011, respectively. He is currently an Associate Professor in mechatronics and the Head of the program for mechatronics engineering at SDU. His research focus is on modeling of mechatronic systems, including solutions of partial differential equations for wave-related phenomena and piezoelectric effect in nano, micro, and macroscopic scales.



His previous industry work includes defense, automotive manufacturing, and design for consumer products and industrial equipment.

**BRIAN VUKSANOVICH** received the B.E. and M.S. degrees in mechanical engineering from Youngstown State University, in 1992 and 1996, respectively. He is currently an Associate Professor in mechanical engineering technology with Youngstown State University. His research areas include automation, advanced manufacturing, as well as ballistics and high strain rate response of materials. His research sponsors include AFRL, ARL, ONR, DOT, and industry.



been funded through the US Department of Transportation, the Department of Defense, NASA, National Science Foundation, and the Ohio Federal Research Network. He has served twice as a Faculty Fellow of the Wright-Patterson Air Force Base.

**PEDRO CORTES** is currently an Associate Professor with the Department of Civil/Environmental and Chemical Engineering program, as well as in the materials science and engineering program with Youngstown State University. He has research interests in the area of 3D printing, including smart and multifunctional materials, composite structures, and metal-ceramic systems. He has published several articles in the area of composite structures and 3D printing. His research work has



acquired by Magma Design Automation Inc., Milpitas, CA, USA. He has spent 2003 to 2016 at the University of Texas at El Paso as the Associate Director of the W. M. Keck Center for 3D Innovation and held faculty fellowships at NASA's Jet Propulsion Laboratory, SPAWAR Navy Research (San Diego), and a State Department Fulbright Fellowship in South America. His research interests include 3D printed multifunctional applications and closed-loop control in additive manufacturing for improved quality and yield. His recent projects include 3D printing of structures such as nano-satellites with electronics in the structure (one of which was launched into Low Earth Orbit, in 2013, and a replica of which is on display at the London Museum of Science). He has over 50 peer-reviewed publications, several patents (one of which was licensed by Sony from IBM). He is a member of the ASEE and a registered Professional Engineer in Texas.

**ERIC MACDONALD** (Senior Member, IEEE) was born in Hokkaido, Japan. He received the Ph.D. degree in electrical engineering from the University of Texas at Austin, in 2002. He is currently a Professor of electrical and computer engineering and is the Friedman Chair for manufacturing at Youngstown State University. He worked in industry for 12 years at IBM and Motorola, Austin, TX, USA, and subsequently co-founded a startup, Pleiades Design and Test, Inc., which was

...